Fuel Communications 18 (2024) 100101

Contents lists available at ScienceDirect

Fuel Communications

journal homepage: www.sciencedirect.com/journal/fuel-communications

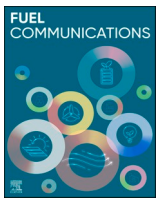

Effects of transition metal doping on the properties and catalytic performance of ZSM-5 zeolite catalyst on ethanol-to-hydrocarbons conversion

Ifeanyi Michael Smarte Anekwe [a,*], Bilainu Oboirien [b], Yusuf Makarfi Isa [a]

[a] School of Chemical and Metallurgical Engineering, University of the Witwatersrand, Johannesburg 2050, South Africa
[b] Department of Chemical Engineering Technology, University of Johannesburg, Johannesburg, South Africa

ARTICLE INFO

Keywords:
Catalyst
Ethanol
Transition metals
Zeolite
ZSM-5

ABSTRACT

In this study, the effects of transition metal-doping on the physicochemical properties and catalytic performance of HZSM-5 catalysts for the conversion of ethanol to hydrocarbons are investigated using experimental data and secondary data from the literature. Hydrothermally synthesized novel ZSM-5 catalysts were modified with different concentrations (0.5 and 10 wt%) of transition metals (Co, Fe, Ni). Characterizations, including X-ray diffraction, Fourier transform infrared spectroscopy, scanning electron microscopy, energy dispersive X-ray spectroscopy, particle size distribution, N_2 adsorption and NH_3 temperature-programmed desorption, revealed the changes in catalyst properties. The introduction of transition metals affected the surface area, particle size and acidity without altering the MFI structures. In particular, a reduction in surface area was observed, ranging from 2.6 to 23 %, corresponding to the different metal loading of 0.5–10 wt% compared to the surface area of the pure catalyst (397.5 m^2/g). In addition, metal-doping led to an increase in Lewis acid sites, accompanied by a decrease in strong acid sites. Catalytic evaluation at 350 °C and a space velocity of 12 h^{-1} showed improved performance in metal-doped ZSM-5 catalysts, which exhibited high selectivity towards fuel-range hydrocarbons, compared to the unmodified catalyst. Catalysts with low metal doping showed optimal catalytic activity, while high metal doping led to increased coke deposition and deactivation of the catalyst due to an increased concentration of strong acids. These results underline the suitability of metal-modified ZSM-5 for hydrocarbon reactions and provide valuable insights for the optimization of catalysts for ethanol conversion to fuel-range hydrocarbons.

1. Introduction

One of the most used solid zeolite acid catalysts is ZSM-5. This catalyst is used in the petrochemical industry in a variety of ways, including the improvement of fuel properties and the production of petrochemicals. ZSM-5 has gained significant recognition in catalysis processes due to the extensive acid sites accessible on the material. In addition, it is overlapping 10-member ring micropores (5.5 Å × 5.1 Å; 5.3 Å × 5.6 Å) justify its acceptable specificity and coke-resistant strength [1]. The building blocks of these zeolites are crystalline networks of SiO_4 and AlO_4 components arranged in a three-dimensional structure with a tetrahedral geometry. In each cross-section of the ZSM-5 structures, elliptical and straight pores are present, which overlap at right angles in a zigzag pattern. After the application of ZSM-5 in some processes, a charge imbalance occurs between the ions in the structures, especially between the Si and Al ions. The properties of ZSM-5 are significantly affected by several variables, including alkalinity, chemical content of the synthesis gel, template, Si/Al ratio, duration of crystallisation, temperature, zeolite manufacturing technique (stationary or rotating environment), incorporation of metals, and other operational variables common to the hydrothermal process [1,2].

ZSM-5 catalysts have proven to be useful in hydrocarbon reactions. The performance and product selectivity of these catalysts can be improved by suitable addition of metallic or non-metallic elements depending on the target product. Metal modification can affect the physiochemical properties of the, and the extent depends on the amount of metal species. However, it should be noted that the modification of ZSM-5 with metal species can increase the tendency of carbon

* Corresponding author.
E-mail address: anekwesmarte@gmail.com (I.M.S. Anekwe).

https://doi.org/10.1016/j.jfueco.2023.100101
Received 7 October 2023; Received in revised form 14 November 2023; Accepted 2 December 2023
Available online 10 December 2023

deposition on the ZSM-5 surface, which reduces the stability and performance of the catalysts. This is the main challenge with ZSM-5 zeolites that impact commercial processes. It is necessary to use a suitable modification strategy to produce zeolites that have fundamental properties . In the context of ethanol-to-hydrocarbon (ETH) conversion, research into the incorporation of metals into HZSM-5 is an area of investigation that includes metals such as Ni, Fe, Zn, Ga, Mo and rare earth metals. In particular, Ni has been observed to improve the conversion of ethanol to higher hydrocarbons by influencing the balance of acid sites and, subsequently, the product distribution. On the contrary, it has been reported that the incorporation of Ga in HZSM-5 increases the production of aromatics, while Fe doping limits the synthesis of aromatics and kerosenes. These effects are attributed to their influence on hydrogen transfer processes [3,4]. Moreover, Zheng et al. [4] reported that doping ZSM-5 with Ga, Zn, Ni, Co, Mg or Cu in the conversion of biomass to aromatics increased the gas yield while decreasing the liquid yield; with Ga-ZSM-5 catalysts, they were able to achieve maximum hydrocarbon yield and minimum coke formation. The study concluded that a Ni- and Co-based catalyst increases benzene and indene production, respectively [4]. To improve catalytic performance and product yield, it is therefore important to dope the catalyst with a suitable amount of metal species [5].

However, other studies in the literature take an opposite view on the effects of metal modification. For instance, Persson et al. [6] reported that loading ZSM-5 with Fe or Ni resulted in a significant coke deposit on the catalyst. They found that the incorporation of Ni or Fe on ZSM-5 improved the yield of MAH, as Ni/ZSM-5 was active in the production of naphthalene [6]. Evaluating the efficiency of a catalyst in the presence of metals is challenging due to variations in reaction parameters, metal concentrations and deactivation. Consequently, the effects of metal incorporation on catalyst properties, reaction mechanisms and product selectivity, particularly C_5+ specificity, remain a poorly understood area. Although these studies investigated the effects of metal doping on ZSM-5 catalysts, some studies used commercially available catalysts, while others did not investigate ethanol conversion at high metal loading ($>$ 5 wt%) and did not study the effects of the various metals on ZSM-5 catalyst properties and product distribution specifically in ethanol conversion into liquid hydrocarbons.

Therefore, this study aims to investigate the effects of selected transition metals on ZSM-5 catalyst properties (including crystallinity, functional groups, textural features – surface area, total pore volume, pore diameter and distribution) and catalytic performance in hydrocarbon reaction. This involves the synthesis, characterisation, promotion, and evaluation of newly fabricated ZSM-5 catalysts. Based on experimental and secondary data from the literature, this study systematically evaluated the changes in the characteristic features of ZSM-5 catalysts before and after (low and high) metal modification (0.5 and 10 wt.%). In addition, the doping effect of the catalyst in ethanol conversion into hydrocarbons was discussed, which allows appropriate conclusions to be drawn about how the properties and activities of the ZSM-5 in catalytic processes are affected by the presence of different transition metal promoters. This study provides researchers and petrochemical industries with useful background on the detailed effects of metals on catalyst properties, performance, and product distribution, enabling the synthesis and effective modification of the required catalyst for the selective production of the target product.

2. Materials and methods

2.1. Materials

Materials used for this study includes $Na_2OsiO_2.H_2O$, $Al_2(SO_4)_3{\cdot}18H_2O$, $C_{12}H_{28}BrN$, NaOH (97 %), H_2SO_4 (98 %), NH_4NO_3, $Ni(NO_3)_2{\cdot}6H_2O$, $Fe(NO_3)_2{\cdot}9H_2O$, $Co(NO_3)_2{\cdot}6H_2O$ and C_2H_5OH. All chemicals were analytical grade obtained from Sigma Aldrich. A stainless-steel hydrothermal reactor (HTR) with a Teflon lining of 200 ml with 150 ml working volume was used for catalyst synthesis.

2.2. Catalyst preparation

The present study employs both experimental and secondary data to evaluate the effects of transition metal modifications on characteristic properties and the activity of the ZSM-5 catalyst. Secondary data were obtained from relevant previous studies. Experimental data were obtained from the present study's catalyst synthesis, characterisation and catalytic test. ZSM-5 was synthesised hydrothermally using the batch formula: $10Na_2O : 40SiO_2 : 1.0Al_2O_3 : 10.5TPABr : 3740{\cdot}6H_2O$. An appropriate amount of chemicals was added, and the pH was stabilised to 10.73 using 99 % concentration of sulfuric acid. The solution was agitated and aged for 6 and 12 h, respectively. The prepared gel was transferred to the HTR for crystallisation at 180 °C for 24 h. After the crystallisation, the solute was obtained by filtration, dried at 110 °C overnight and calcined at 550 °C for 3 h to eliminate the organic template. The as-synthesised Na-ZSM-5 was ion-exchanged using a 1 M solution of NH_4NO_3 at 10 ml/g catalysts. The process was repeated two times to obtain NH_4-ZSM-5 and calcined at 550 °C for 6 h to obtain the HZSM-5 used for the present study. The catalyst was modified using transition metals (M = Co, Fe and Ni) at 0.5 wt% and 10 wt% through incipient wetness impregnation and calcined at 550 °C for 6 h. Transition metal-modified ZSM-5 were denoted xM and yM, where x and y represent 0.5 and 10 wt% of transition metal (M), respectively.

2.3. Catalyst characterisation

Using an X-ray diffractometer (Bruker D2 Phaser Diffractometer) equipped with Cu K radiation [λ = 1.54184 Å], the crystallinity of the catalyst was analyzed in $2\theta = 0–90°$ at 0.02° and a counting time of 31.4 s per step. Infrared spectra (IR) were recorded at room temperature using a Perkin Elmer Fourier Transform-Attenuated Total Reflectance - Infrared Spectrometer Sprecrum-2 (FT-ATR-IR -2) range 4000–400 cm^{-1}. This made it possible to determine the functional groups. Using a ZEISS Sigma 300 VP, equipped with a field emission gun for the scanning electron microscope (SEM) and Oxford Instruments x-act PentaFET Precision Energy-dispersive X-ray spectroscopy (EDS), the morphology of the catalyst and a semi-quantitative characterisation of its elemental composition was determined. Surface areas and pore volumes were obtained from N_2 adsorption-desorption measurements (Quantachrome Instrument: Autosorb iQ Station 3, Anton Paar, USA) (estimated using the Brunauer, Emmett and Teller (BET) and Barrett, Joyner, and Halenda (BJH) techniques, respectively) performed after the sample had been outgassed under vacuum at 300 °C for 10 h. The Malvern instrument was used to obtain the particle size distribution (PSD) data. Gas chromatography was employed for the analysis of hydrocarbon products (GC). NH_3-TPD analysis was conducted using an AutoChem II 2920 chemisorption analyzer to determine catalyst acidity. The adsorbed water was eliminated by heating the sample at 300 °C at 10 °C/min until reaching a temperature of 700 °C, during which a TCD detector was employed to measure the desorption NH_3 signal.

To evaluate the thermal properties of the catalyst after the reaction, thermogravimetric analysis (TGA) was performed using TA Instruments Q50, USA. This was to monitor the amount of coke deposited. To remove moisture and unbound volatile compounds, the samples were heated in a nitrogen stream from room temperature to 200 ℃ with a ramp rate of 15 ℃ per minute and a flow rate of 50 ml per minute. After that, the N_2 gas stream was replaced by an air stream and the temperature was increased to 800 ℃ while maintaining the same flow rate.

2.4. Catalyst evaluation

The catalytic conversion process was carried out in a fixed-bed reactor at 350 °C, a weight hourly space velocity (WHSV) of 12 h^{-1} and two hours time-on-stream (TOS). The catalyst bed was supported

using glass beads and glass wool of 0.045 g. Ethanol was used as the feedstock for the reaction, which was fed to the reactor with the HPLC pump after 40 min of catalyst activation at 400 °C.

3. Results and discussion

3.1. Effect of transition metal modification on the crystallinity of ZSM-5

All the XRD patterns of synthesised materials showed the characteristic peak of the standard ZSM-5 catalyst. The XRD result revealed that the characteristic peaks were observed for both the original and the transition metal-doped catalyst at 2θ = 7–9° and 23–25°. Distinctive diffraction peaks were observed at 7.97°, 8.88°, 14.81°, 23.14°, 23.32°, and 24.00° assigned to reflective planes (101), (020), (301), (501), (303) and (133) of the MFI framework of the ZSM-5 catalyst (Fig. 1) (ICDD 96-154-02,468). The fact that the XRD patterns do not contain any other unexplained peaks is evidence that amorphous SiO_2 did not form simultaneously with ZSM-5. The absence of promoter-related peaks in the XRD patterns of some modified catalysts is due to the presence of transition metal promoter in a small amount (0.5 wt% of Co, Fe and Ni), which suggests the presence of doped metal in small amounts or an unusually uniform distribution of the incorporated metal during the doping process [4]. The height of the peak ratio at 2θ = 22.5–25.0° compared to the peak area of the pure catalyst is the definition of relative crystallinity, determined according to ASTM [7]. Since the increased loading of transition metals lowers both the intensity and peak area, the impregnated HZSM-5 catalysts exhibit lower relative crystallinity, with a loading of 10 wt.% Co, Fe, and Ni compared to a loading of 0.5 wt% and an unmodified catalyst.

The chemical states of metal species on the doped catalysts are revealed by the characteristic peaks of the metal oxides, including Cr_2O_3, Fe_{2O_3}(haematite), NiO particles on the ZSM-5 surface (corresponding to the oxidation state of Cr^{3+}, Fe^{3+} and Ni^{2+}, respectively). These peaks of metal oxides were prominent in high metal loading. The peak at 37.2°, 43.3° and 62.9° corresponds to NiO assigned to ICDD 96-432-9324, and the peaks at 33.2° and 35.8° and 49.2° are attributed to Fe_2O_3 (ICDD 00-024-0072), while Co_3O_4 corresponds to the peaks at 31.7°, 36.9° and 65.4° (Supplementary Information, *SI.* Fig. 1) which corresponds to ICDD 96-153-8532. Before and after the modification, all the catalysts had MFI framework and showed diffraction peaks of ZSM-5 [8]. Thus, the framework of ZSM-5 was successfully preserved despite introducing transition metals. This is evidence that the catalyst in question has a ZSM-5 zeolite framework. However, a reduction in percentage crystallinity was recorded with the modification of transition metals and a further decrease in the characteristic peak with increased percentage doping [8]. The comparative evaluation of the XRD characterisation of the relative degrees of crystallisation (RDC) of different ZSM-5 catalysts doped with transition metals was calculated and presented in Table 1, using the four significantly stronger diffraction peaks of unmodified HZSM-5 at 2θ = 7°–9° and 23°–25° as reference points. Notably, the percentage relative degree of crystallisation (RDC) of each of the doped catalysts either increased or decreased due to the modification process. According to Machado et al., the RDC of the (4.8 wt%) Fe/ZSM-5 catalyst reduced drastically to 60 %, while the RDC of the (0.25 wt%)Fe/HZSM-5 catalyst increased slightly to 114 %, attributed to high and low metal-doping, respectively [9]. It can be deduced that the type of transition metal and increased loading leads to a loss in structural orderliness, as seen by the lower relative degree of crystallisation.

In agreement with the present study, Li, et al. [10] reported from the XRD of the metal-doped (5–10 wt%) samples the presence of metal oxide was discovered after careful inspection of the patterns (peaks) in the range of 2θ = 35.6° and 38.7° for CuO [11]; 2θ = 37.2° and 43.3° for NiO and 2θ = 33.6°, 36.1° and 41.5° for Cr_2O_3 [12]. The peaks in these samples indicated the formation of transition metal oxides. With respect to YZM, it was found that there were no conspicuous peaks within the

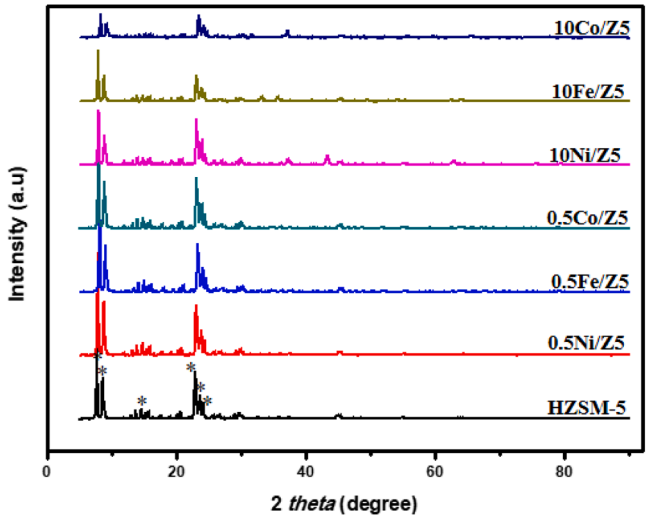

Fig. 1. XRD patterns of pure and transition metal-modified HZSM-5 catalysts.

Table 1
Comparing the sum of intensities of transition metal doped HZSM-5 with that of pure HZSM-5.

Catalysts	% Metal loading	Relative crystallisation (XRD)%	Refs.
HZSM-5 (Si/Al = 40)	0	Ref. pattern	Present Study
0.5Co/Z5	0.5	85.7	
0.5Fe/Z5	0.5	85.6	
0.5Ni/Z5	0.5	99.9	
10Co/Z5	10	43.7	
10Fe/Z5	10	57.1	
10Ni/Z5	10	71.4	
HZSM-5	0	Ref.	[9]
Fe/Z5	0.25	114	
Fe/Z5	0.25	108	
Fe/Z5	0.33	108	
Fe/Z5	0.33	105	
Fe/Z5	4.8	60	
Fe/Z5	4.7	80	
Fe/Z5	5.0	80	
HZSM-5	0	Ref.	[8]
Cu/Z5	3	88.4	
La/Z5	3	77.9	
Zn/Z5	3	48.6	
ZSM-5	0	90	[15]
Mn/Z5	Mn (4)	67.5	
Mn–Cr/Z5	Mn-Cr (4–0.93)	79.2	
Mn–Mn/Z5	Mn-Mn (4–0.98)	70.2	
Mn–Fe/Z5	Mn-Fe (4–1)	56.7	
Mn–Co/Z5	Mn-Co (4–1.05)	56.7	
Mn–Ni/Z5	Mn-Ni (4–1.05)	73.8	
Mn–Cu/Z5	Mn-Cu (4–1.14)	50.4	
Mn–Zn/Z5	Mn-Zn (4–1.17)	57.6	
Ga/Z5	5 %Ga	Ref.	[16]
$Ga/Z5_{0.2M}$	5 %Ga0.2 % NaOH	94.7	
$Ga/Z5_{0.6M}$	5 %Ga0.6 % NaOH	90.3	
$Ga/Z5_{0.8M}$	5 %Ga0.8 % NaOH	82.4	
$Ga/Z5_{1.0M}$	5 %Ga1.0 % NaOH	72.9	
ZSM-5 (Si/Al=20)	0	Ref.	
Fe/Z5	0.5	89	
Fe/Z5	0.25	90	[14]
Fe/Z5	4.8	95	
Fe/Z5	1.82	97	
Fe/Z5	5	98	

studied angles, suggesting either the absence of yttrium oxide or an exceptionally uniform distribution of Y metal species [13]. Considering that there was no significant shift in the intensity of the diffraction peaks between the several molecular sieves, it was concluded that the framework of the ZSM-5 molecular sieve was not affected. It should be noted that the differences in crystallinity can also be attributed to the synthesis method and post-treatment techniques applied to these catalysts [14].

3.2. Effect of transition metal modification on the functional groups of ZSM-5 catalyst

The FTIR analysis is usually performed in the 400–4000 cm^{-1} range to identify functional groups in the synthesised materials, such as the ZSM-5 zeolite catalyst. The FTIR result shows that the pure and transition metal-doped ZSM-5 exhibit characteristic peaks of the functional groups of ZSM-5 represented by different bands (Fig. 2). However, increased metal doping from 0.5 to 10 wt.% Co, Fe and Ni resulted in decreased intensity, and different peaks represented the presence of metal oxides at high loading. The decrease in peak intensity at high loading (10 wt.%) follows the pattern: Co < Fe < Ni. The crystalline framework of the zeolite is revealed by the strength of the bond at ~400 and 500 cm^{-1}. The band at 440 cm^{-1}corresponds to the stretching of T-O bonding of the internal tetrahedral of SiO_4 and AlO_4 units, while the pattern of peaks at ~543 cm^{-1} depicts the vibrational intensity of the double five-member ring in the MFI framework of the ZSM-5 catalyst [17]. The intense peak in the region of 791–1064 cm^{-1} is due to the internal asymmetrical stretching vibration between the Si-O-Si bonds [18], which depends on the Si/Al ratio; a decrease in the ratio of this peak results in a shift to lower values while the peak at 1218 cm^{-1} is attributed to external asymmetrical stretching. A peak denotes the adsorbed H2O on the catalyst surface at 1633 cm^{-1} [17]. The IR spectrum in the range 3000–3900 cm^{-1} corresponds to the vibration and elasticity of the O—H bonds [19]. However, the bands at about 3646 cm^{-1} identify the hydroxyl groups on extra framework Al and strong Brønsted acid sites (Si-Al-OH) [17]. The metal oxides (for 10 wt% metal species) are attributed to the 661, 545, and 670 cm-1 peaks, representing Co_3O_4, Fe_2O_3 and NiO, respectively [20–22]. It can also be seen from Fig. 2 that the loading of 10 wt% Ni on the ZSM-5 causes the most

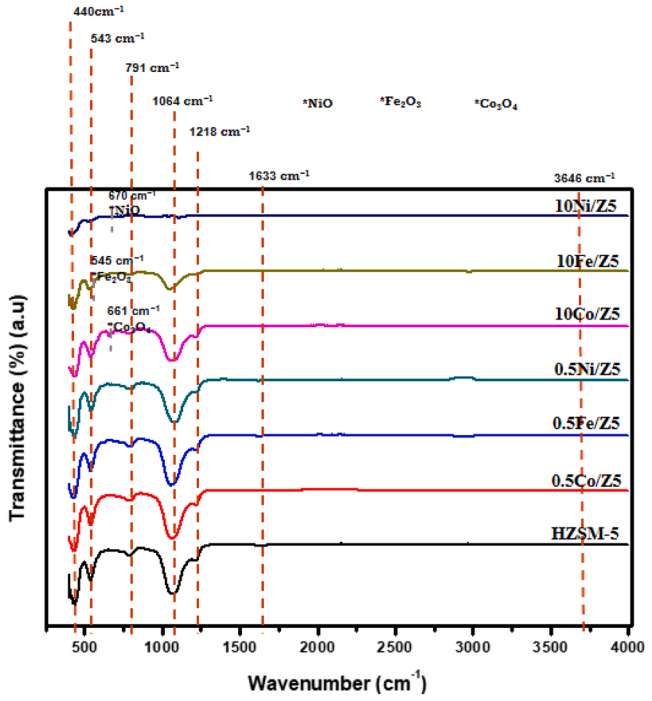

Fig. 2. FTIR spectra of pure and transition metal-doped HZSM-5 catalysts.

absorption bands in the region of 400–4000 cm^{-1} to drop drastically and nearly completely disappear. Owing to the small concentration of 0.5 wt % metal doping, the FTIR results on these samples did not show any clear peaks of the oxide [10].

Table 2 shows the absorbence at wavelengths 540 and 450 cm^{-1} and illustrates that modification of the transition metals can lead to a decrease or increase in FTIR crystallinity at these peaks, depending on the metal type and concentration. The intensity ratio (also known as IR crystallinity) of the peaks at 540 and 450 cm^{-1} is due to the evolution of the MFI zeolite, except for 0.5 wt.% Fe loading with other transition metals reduced the intensity of the 450 and 540 cm^{-1} peaks, with higher loading (10 wt.%) leading to a significant decrease in these peaks. The present study agrees with the study by Calsavara et al. [14], who found a decrease in the absorbence at 540 and 450 cm^{-1} wavelengths with the introduction of transition metals. However, Saeidi and Hamidzadeh [15] noted that the strength of the peak was increased by incorporating Mn and co-doped metals, confirming that the number of Brønsted acid sites was increased [15]. This shows the different effects of transition metals with regard to a decrease in IR crystallinity.

3.3. Effect of transition metal modification on morphology and particle size of HZSM-5 catalyst

Images from SEM analysis show a spherical aggregate largely homogeneous for both parent catalysts and catalysts doped with transition metals (Fig. 3). Images taken with a high-resolution scanning electron microscope show nanoscale crystals aggregating into microspheres. Due to the higher nucleation density, delayed crystallisation, and aggregation after nucleation, smaller particles may be visible on the microspheres [18]. The SEM result showed that the catalyst consists of

Table 2
Comparing the absorbence/transmittance at 550 and 450 cm^{-1} of transition metal-doped with that of pure ZSM-5.

Sample	Transition metal content (%)	Peak Intensity, FTIR (%) I_{450}	Peak Intensity, FTIR (%) I_{540}	I_{450} / I_{540}	Refs.
HZSM-5	0	Ref.	Ref.	1.00	Present study
0.5Co/Z5	0.5	99.1	98.5	0.994	
0.5Fe/Z5	0.5	102.7	101.5	0.989	
0.5Ni/Z5	0.5	93.8	90.9	0.970	
10Co/Z5	10	83.9	86.4	1.029	
10Fe/Z5	10	60.7	53.0	0.873	
10Ni/Z5	10	29.4	15.2	0.514	
Mn/ZSM-5	Mn (4)	67.0	62	0.925	[15]
Mn–Cr/ ZSM-5	Mn-Cr (4–0.93)	57	50	0.877	
Mn–Mn/ ZSM-5	Mn-Mn (4–0.98)	72	66	0.917	
Mn–Fe/ ZSM-5	Mn-Fe (4–1)	62	57	0.919	
Mn–Co/ ZSM-5	Mn-Co (4–1.05)	70	66	0.942	
Mn–Ni/ ZSM-5	Mn-Ni (4–1.05)	76	72	0.947	
Mn–Cu/ ZSM-5	Mn-Cu (4–1.14)	68	65	0.956	
Mn–Zn/ ZSM-5	Mn-Zn (4–1.17)	72	66	0.917	
Fe/Z5	0.02	Ref.			[14]
Fe/Z5	4.7	95			
Fe/Z5	5.0	98			
Fe/Z5	0.25	95			
Fe/Z5	0.25	90			
Fe/Z5	0.33	90			
Fe/Z5	0.33	97			
Fe/Z5	4.8	91			
Fe/Z5	4.8	95			

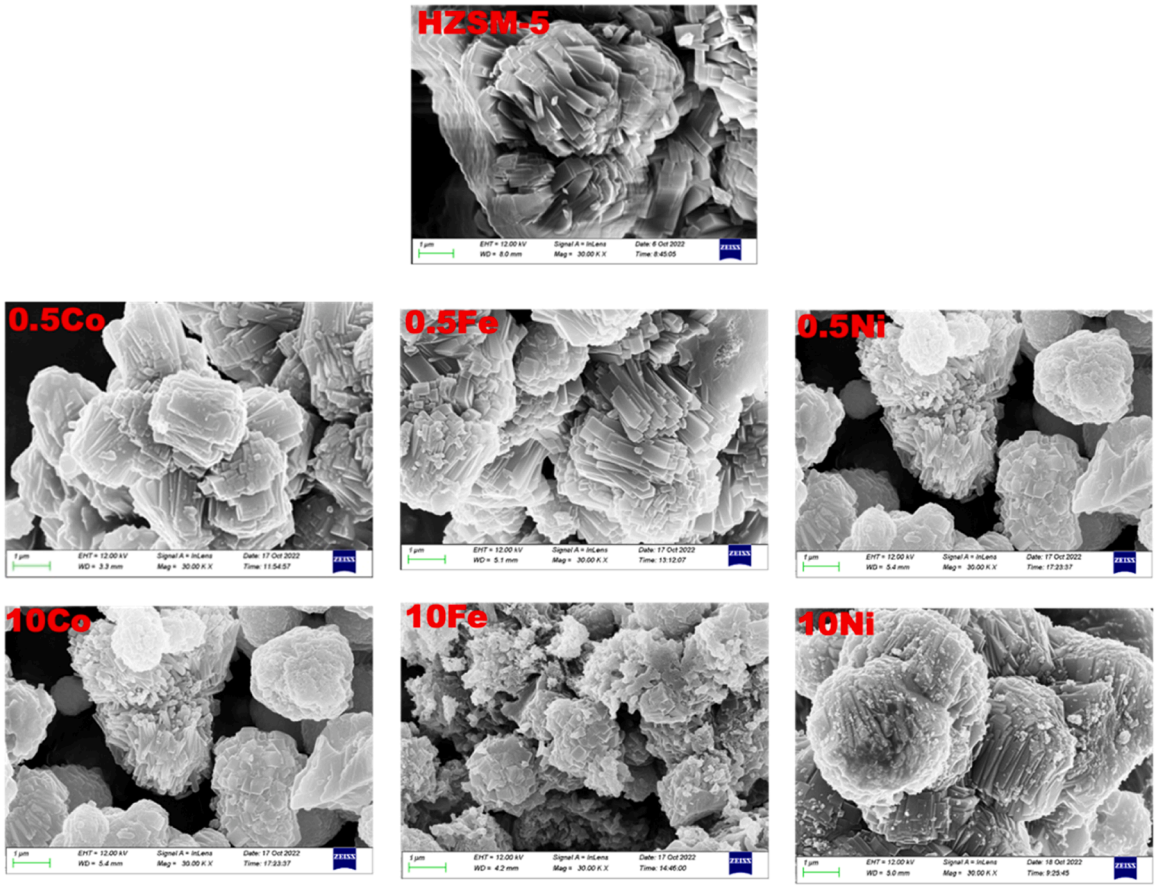

Fig. 3. SEM images of pure and transition metal-doped HZSM-5.

prismatic crystals of MFI structure, which agrees with the result obtained from the XRD pattern [23]. After impregnation, the morphology of the crystal showed no signs of significant changes. Also, the Si/Al ratio did not change during the impregnation process, which is further evidence that the impregnation process did not affect the overall composition of the zeolite framework [24]. When the metal promotion was performed at a concentration of 10 wt%, an unusual side effect occurred: some of the promoters precipitated on the catalyst surface, which could be observed in the EDS spectrum (*SI.* Fig. 2). The change in the morphology of the ZSM-5 catalyst with metal loading can be attributed to several factors. The presence of transition metal ions can affect the nucleation and growth of ZSM-5 crystals. Fig. 3 shows that different metals can interact differently with the crystal growth sites of ZSM-5, resulting in variations in crystal size, shape, and orientation. It is also noted that transition metals have different atomic sizes and charge densities. When incorporated into the ZSM-5 lattice, they can disrupt the regular crystal structure and affect the arrangement of Si and Al atoms in the zeolite framework. Depending on the amount of metal incorporated, this can lead to the formation of metal-containing clusters or domains within the zeolite structure, which can alter its morphology. Hence, the concentration of the metal dopant can significantly affect the zeolite's morphology. As shown in the images from SEM, at lower concentrations (0.5 wt%), the metal ions may be more evenly distributed in the zeolite lattice, resulting in subtle changes in morphology. At higher concentrations (10 wt%), the metal ions may cluster together, resulting in more pronounced surface morphological changes [25].

The results of the PSD analysis, shown in *SI.* Fig. 2, indicate that the particle size distribution for HZSM-5 and metal-doped catalysts ranges from 0.5 to 50 and 0.5–1000 μm, respectively. The introduction of transition metal species leads to a bimodal distribution, indicating different growth processes, particle fragmentation and the presence of larger particles in the system. Thus, metal doping affects the particle size, which is due to the precipitation and aggregation of the metal species and their interaction with the zeolite framework. Consequently, the particle size of the doped HZSM-5 tends to increase (with respect to the particle size of the initial HZSM-5, 4.55 μm) with an increase in metal doping from 0.5 to 10 wt%. The average particle size of 0.5Fe and 10Fe increases by 1.19 and 6.93 μm; 0.5Ni and 10Ni increases by 1.78 and 8.67 μm; 0.5Co and 10Co increases by 0.19 and 4.31 μm. This may be due to the penetration of the metal species into the pores and channels of the zeolite during the impregnation process [26]. The EDS spectrum showed the presence of transition metals (Co, Fe and Ni) at 10 wt% in the modified catalysts (*SI.* Fig. 3).

3.4. Effect of transition metal modification on the surface area and porosity of ZSM-5

The specific surface area of the catalyst (S_{BET}) is another important factor for catalytic activity. Table 3 shows the results of the various BET analyzes (surface area, pore volume and pore size distribution) from the present and other studies on ZSM-5. It is evident from Table 3 that the modification of transition metals decreases the surface area and total pore volume of the modified catalysts. In the present study, it was observed that the surface area of the synthesised material decreases from 397.5 (for pure ZSM-5) to 362.6, 387.2 and 381.6 m^2g^{-1} for 0.5 wt% and 319.3, 348.0 and 306.2 m^2g^{-1} for 10 wt% Co, Fe and Ni, respectively. The increased doping of 10 wt% of transition metals further reduces the respective surface area of the modified catalysts (S_{BET}). It was observed that the ZSM-5 synthesised in the present study has a significant surface area (397.5 m^2g^{-1}) compared to other studies investigated, as shown in Table 3. Similarly, the total pore volume decreases with metal loading from 0.71 (of pure ZSM-5) to 0.46, 0.45 and 0.59 cm^3g^{-1} for 0.5 wt%

Table 3
Review of results of different BET analyzes on the effect of transition metal modification on the surface area, pore volume and pore size distribution of the ZSM-5 zeolite catalyst.

Catalysts (Si/Al)	S_{BET} (m^2g^{-1})	S_{micro} (m^2 g^{-1})	S_{ext} (m^2 g^{-})	V_{total} (cm^3 g^{-1})	V_{micro} (cm^3 g^{-1})	V_{meso} (cm^3 g^{-1})	Avg pore dia. (nm)	Metal (wt%)	MDM/ Refs.
HZSM-5 (40)	397.5	335.2		0.706	V_{meso} 0.678	V_{macro} 0.0285	2.224	0	DIM
0.5Co/Z5	362.6	312.4		0.461	0.456	0.0057	2.008	0.5	
0.5Fe/Z5	387.2	331.4		0.449	0.448	0.0006	1.999	0.5	Present
0.5Ni/Z5	381.4	318.9		0.710	0.709	0.0001	2.024	0.5	study
10Co/Z5	319.3	261.3		0.420	0.405	0.0147	1.919	10	
10Fe/Z5	348.0	289.8		0.701	0.668	0.0325	2.497	10	
10Ni/Z5	306.2	250.0		0.663	0.663	0.0002	2.681	10	
ZSM-5_M	373	214	159	0.300	0.100	0.200		–	MSG
Cr/Z5	286	180	106	0.219	0.090	0.129		11.62	[27]
Cu/Z5	297	197	100	0.202	0.096	0.106		9.56	
Ga/Z5	318	197	121	0.213	0.096	0.117		10.31	
La/Z5	335	215	120	0.234	0.105	0.129		8.95	
Mg/Z5	229	178	51	0.177	0.087	0.090		8.64	
Y/Z5	293	185	108	0.208	0.090	0.118		10.34	
Ni/Z5	317	195	122	0.217	0.095	0.122		11.05	
Zn/Z5	285	185	100	0.227	0.090	0.137		11.34	
HZSM-5	342.9			0.457			5.9	3	IIM
Cu/Z5	328.2			0.440			6.0	3	[8]
La/Z5	325.3			0.438			6.0	3	
Zn/Z5	326.2			0.437			6.0	3	
ZSM-5 (20)	386			0.25	0.16	0.09	2.41	0	WIM
Mo/Z5	259			0.18	0.10	0.08	2.40	25	[17]
HZSM-5 (25)	338.4	195.6	142.8	0.2861	0.1016	0.1845	3.38	0	WIM
Ga/Z5	293.5	163.6	129.9	0.2467	0.08499	0.1617	3.39	5	[4]
Ni/Z5	291.4	162.9	128.4	0.2488	0.08472	0.1641	3.45	5	
Mg/Z5	282.1	167.7	114.4	0.2448	0.08626	0.1585	3.42	5	
Co/Z5	288.9	161.0	127.9	0.2460	0.08376	0.1622	3.44	5	
Zn/Z5	288.2	167.6	120.6	0.2483	0.08738	0.1609	3.38	5	
Cu/Z5	287.5	166.0	121.6	0.2387	0.08708	0.1516	3.41	5	
Ga/Z5	338		60.1		$V_{meso+macro}$ 0.064			*(Si/Ga)* 5.4	DIM
$Ga/Z5_{0.2M}$	334		64.6		0.092			6	[16]
$Ga/Z5_{0.6M}$	366		106.7		0.156			14	
$Ga/Z5_{0.8M}$	393		134.2		0.238			13.5	
$Ga/Z5_{1.0M}$	421		170.6		0.457			12.5	
ZSM-5(200)	321.11	281.71	39.40	0.19	0.13	0.06		0.5	WIM
Ag/Z5	315.14	276.41	38.73	0.18	0.12	0.06		0.5	[28]
Ir/ Z5	327.35	288.13	39.22	0.19	0.12	0.07		0.5	
Ni/Z5	314.67	272.85	41.82	0.19	0.12	0.07		0.5	

Metal Doping Methods (MDM): MSG – Metal addition in synthesis gel; IIM – Isometric Imprgnation;.
WIM – Wet Impregnation; DIM – Dry Impregnation.

and 0.42, 0.70 and 0.66 cm^3g^{-1} for 10 wt% Co, Fe and Ni loading, respectively. However, the average pore diameter decreased at a loading of 0.5 wt% and increased at a metal loading of 10 wt%. The decrease in S_{BET} and pore volume is due to the formation of metal oxide during the process of transition metal modification, which covers the surface of ZSM-5 and partially blocks the zeolite channels [27]. The slight change in mesoporous volume determined using the BJH approach showed that the decrease in macropore volume mainly caused the decrease in total pore volume. The significant reduction in the volume of the mesopores, which ranged in size from 10 to 50 nm, was the cause of the decrease in the total pore volume. The effect of metal doping on the pore size in the range of 1–5 nm varied depending on the metal and the amount of metal content: 10 wt% Ni, followed by Fe, and then Co showed a larger pore size compared to 0.5 wt% loading of these metals.

The results of this study are consistent with those of previous studies. Li et al. [27] showed that the S_{BET} for Cr/Z5, Cu/Z5, Ni/Z5 and Y/Z5 decreased from 373 m^2g^{-1} to 286, 297, 317 and 293 m^2g^{-1}, respectively. Similarly, the pore volume decreased from 0.300 to 0.219, 0.202, 0.217 and 0.208 cm^3g^{-1} for Cr/Z5, Cu/Z5 and Ni/Z5, respectively. Similarly, Zheng et al. [4] reported that the S_{BET} of the unmodified H-ZSM-5 is considerably high (338.44 m^2g^{-1}) compared to that of the improved ZSM-5, which decreases and ranges between 293 and 287 m^2g^{-1}. The pore volume decreased and the average pore size increased, although the change was minimal. Although part of the zeolite surface is covered and the modifications block some pores, the structural integrity of the material has not changed [8]. The N_2 adsorption–desorption isotherms of the investigated materials in the present study showed that the unmodified ZSM-5 exhibited greater N_2 adsorption than the metal-doped zeolites (Fig. 4). The adsorbed volume increases continuously with the relative pressure and decreases with the metal-doped catalysts. These catalysts exhibited type IV isotherms with hysteresis loops of different diameters corresponding to adsorption-desorption in the mesopores. This is consistent with the study of Ji et al. [8]. In addition to the inherent zeolite channels, the different peaks observed in all samples indicated that the ZSM-5 catalyst has a hierarchical macro-mesoporous structure [27].

3.5. *Effect of transition metals on the acidity of ZSM-5*

The strength and concentration of acidic sites in ZSM-5 catalysts can be determined using the NH_3-TPD assay. Table 4 shows the results of ammonia temperature-programmed desorption (TPD) for pure HZSM-5 and metal-modified HZSM-5 catalysts. The TPD analysis revealed three distinct desorption bands observed at different temperature ranges: 180–200 °C, 400–450 °C and 650–700 °C, corresponding to weak acid, moderate acid, and strong acid sites, respectively. The desorption band in the 180–200 °C range can be attributed to physically and weakly chemically adsorbed ammonia, while the band in the 400–450 °C range

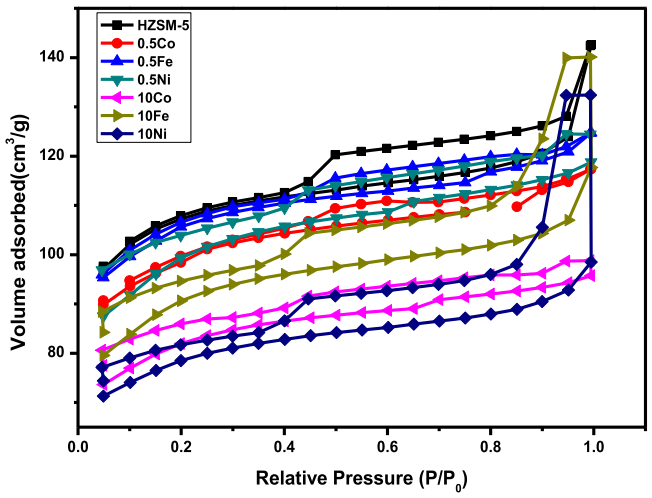

Fig. 4. N_2adsorption-desorption isotherm results for the pure and transition metal-doped HZSM-5 catalysts.

indicates NH_3 adsorbed on the hydroxyl group of zeolites. The 650–700 °C desorption band is associated with dehydroxylation and desorption of NH_3 from the strong Brønsted acid sites or Lewis acid sites [29]. Upon incorporating metal species into HZSM-5, the acid characteristics change, including an increase in the weak acid sites and a decrease in moderate and strong acid sites. These changes in acidity are accompanied by a shift in peak temperatures, which can be attributed to the interaction between the zeolite framework and the metal species. The weak acid sites showed an increase of 9.5 %, 5.9 % and 10.4 % at peak temperatures of 189 °C, 194 °C and 190 °C, respectively, for 0.5 wt % Co-, Fe- and Ni-doped catalysts compared to the unmodified HZSM-5 catalyst with 0.95 mmol/g at 198 °C. Among the metal-doped catalysts, the Ni-doped catalyst exhibited the highest increase in weak acid sites. A substantial increase in metal doping (up to 10 wt%) resulted in a 46.3, 37.9, and 28.4 % decrease in Co, Fe and Ni-doped catalysts. The number of moderate acid sites increased slightly by 6.3 % at a peak temperature of 436 °C for the Fe-doped catalyst, while Co- and Ni-doped catalysts decreased by 6.8 % within this temperature range. While 10 wt% Co and Fe-doped catalysts recorded a decrease (5.4 and 48.6 %) in moderate acid, 10 wt% Ni increased these acid sites by 56.7 %. A significant decrease in the strongly acid sites was observed for all metal-doped catalysts, resulting in decreases of 27.5 %, 29.2 % and 41.7 % for 0.5 wt% catalysts with reference to the unmodified HZSM-5 catalyst except 10 wt% which led to an increase in strong acid sites. However, despite the decline in strong acid sites for low metal-doped catalysts, the modification of transition metals led to an overall increase in the total acidity of the respective catalysts.

The results of the present study are consistent with previous research indicating that the incorporation of transition metals (Co, Fe and Ni) can alter the concentration of acid sites in the catalyst [27]. This effect is primarily due to the electronic interactions between the metal species and the framework of the ZSM-5 zeolite. When metal ions are doped into the ZSM-5 catalyst, they can replace some protons and occupy the cationic positions within the zeolite framework. These ions have a lower positive charge density than protons, resulting in a weaker electrostatic interaction with the oxygen atoms of the framework. As a result, the metal-doped ZSM-5 catalyst exhibits a lower strong acidity as the less acidic metal ions replace the strong acid sites (protons). The weaker acid sites provided by the metal species lead to a decrease in strong acidity with a simultaneous increase in weak acid sites [30]. However, it should be noted that the decrease in strong acid sites is not always desirable, as the catalytic performance of ZSM-5 in some catalytic reactions may depend on the presence of these strong acid sites. In the present study,

Table 4
Effects of transition metals modification on strong and weak acid concentration.

Catalysts	Peak Temp (°C)			Acidity conc. (mmol NH_3/g)					
	L.T.	M.T.	H.T.	Weak	Moderate	Strong	Total acidity	SA/WA	Refs
HZSM-5	198	419	686	0.950	0.74	0.024	1.714	0.025	
0.5Co	189	425	667	1.050	0.690	0.015	1.755	0.014	Present
0.5Fe	194	436	678	1.010	0.790	0.017	1.817	0.017	Study
0.5Ni	190	435	688	1.060	0.690	0.014	1.764	0.013	
10Co	172	438	623	0.510	0.700	0.030	1.214	0.059	
10Fe	168	418	612	0.590	0.380	0.038	1.008	0.064	
10Ni	178	427	617	0.680	1.710	0.060	2.45	0.088	
ZSM-5	182	233	379	0.011	0.039	0.050	0.10	4.58	
Zn/ZSM-5	194	255	365	0.023	0.024	0.053	0.10	2.29	[31]
Fe/ZSM-5	182	236	385	0.011	0.039	0.050	0.10	4.40	
Ca/ZSM-5	193	254	341	0.021	0.051	0.029	0.10	1.41	
Ce/ZSM-5	193	252	383	0.024	0.035	0.041	0.10	1.68	
La/ZSM-5	220	304	444	0.023	0.054	0.023	0.10	1.03	
ZSM-5	207		394	0.42		0.20	0.61	0.50	
Cr/Z5	205		371	0.32		0.14	0.43	0.33	[27]
Cu/Z5	297		459	0.61		0.20	0.81	0.33	
Ga/Z5	207		364	0.43		0.21	0.62	0.50	
La/Z5	209		375	0.42		0.07	0.52	0.18	
Y/Z5	208		364	0.51		0.07	0.61	0.14	
Zn/Z5	213		375	0.53		0.06	0.61	0.12	
ZSM-5	207		394	0.40		0.16	0.56	0.40	
Ni/Z5	216		376	0.55		0.13	0.68	0.24	[10]
Y/Z5	208		385	0.52		0.07	0.59	0.13	
ZSM-5				0.53		0.53	1.06	1.00	
Fe/Z5				0.22		0.21	0.43	0.95	[32]
0.1Fe/Z5				0.43		0.53	0.96	1.23	
0.5Fe/Z5				0.44		0.53	0.97	1.20	
1.0Fe/Z5				0.49		0.53	1.03	1.09	
HZSM-5 (Si/Al=200)				0.51		0.57	1.08	1.11	
Ag/Z5				0.43		0.53	0.96	1.23	[28]
Ir/Z5				0.52		0.69	1.21	1.32	
Ni/Z5				0.52		0.51	1.03	0.98	

LT – Low temperature; MT – Medium temperature; HT – High temperature; SA/WA – Strong acid/Weak acid.

the intentional incorporation of metal species aims to modify the catalytic behavior of ZSM-5 and provide alternative reactions or selectivity that are not solely dependent on the strong acid sites.

3.6. Effect of transition metal modification on catalytic performance of ZSM-5 in hydrocarbon reaction

Ethanol conversion over HZSM-5 and metal-doped catalysts in the present study at $T = 350$ °C and WHSV=12 h^{-1} recorded >97 % conversion for all catalysts studied (Fig. 5). Different types of hydrocarbons (HCs) are present in the products of the ZSM-5 before and after doping with transition metals. All catalysts showed a varying product distribution, including C_1—C_4, C_5—C_8, C_9—C_{12}, C_{12}+ and aromatics (benzene). Due to the reaction conditions employed, more liquid than gaseous products is found in the product distribution. This can be explained by the WHSV, which determines the duration of contact with the catalyst; for example, a higher WHSV means a higher flow rate and, consequently, a shorter duration of contact with the catalyst. The less contact the hydrocarbon has with the catalyst, the fewer side reactions occur, which should ultimately lead to higher chain hydrocarbon selectivity [33]. However, while the unmodified catalyst did not show C_9—C_{12} hydrocarbons in the product distribution, modified catalysts (mostly 0.5 wt% Co and Fe) showed appreciable amounts that decreased with increased metal concentration (from 0.5 to 10 wt%) from 38.6 to 1.9 %. The 0.5 wt%Fe catalysts recorded the lowest gaseous products (C_1—C_4) of ~4 %, which can be attributed to the conversion of these products into liquid HCs (mainly C_9—C_{12}). The transition metal doped (0.5 wt% Ni and 10 wt% Co) ZSM-5 favoured benzene (5 and 4 %) and C_5—C_8 (48.4 and 41.2 %) HC production with selectivity, while 0.5 and 10 wt% Fe were the most selective for C_9—C_{12} (38.6 %) and C_{12}+ (70.2 %) HCs compared to the other catalysts. The enhanced activity of modified catalysts can be due to the weak crystal framework of transition metal oxides, which can increase oxygen vacancy and improve catalytic activity [34]. This agrees with the study by Persson et al. [35], which showed that metal modification improved the amount of aromatic HCs in the liquid product, especially monoaromatic HCs (MAH) and naphthalenes, from 59 to 83 %. While Ni also favoured naphthalenes, Fe primarily improved the specificity of MAHs compared to unmodified ZSM-5 [35]. To further bolster the effect of transition metal, Huang et al. [36] reported that adding Ni, Fe, or Co has little effect on catalytic performance but alters the product distribution. Despite an increase in ethylbenzene, the content of non-aromatics and aromatics increased relative to Fe/HZSM while Ni increased, especially the aromatic content.

The role of the metal species in the doped catalysts in product selectivity and distribution varies depending on the type and concentration of the metal species. For metal-doped ZSM-5 catalysts, the improved performance of the doped catalysts can be attributed to the presence of metal species that actively participate in the hydrocarbon (HC) reaction. When metal species are introduced into the ZSM-5 framework, they alter the properties of the catalyst, as described in the previous sections, and the catalytic performance. The interaction between the metal species and the zeolite framework leads to synergistic effects, where the combined properties of the metal and zeolite result in improved catalytic performance, as evident in product distribution (Fig. 5). Compared to unmodified catalysts, the metal species (Co^{2+}, Fe^{3+}, and Ni^{2+}) present in the metal-doped catalysts play a crucial role in promoting the formation of intermediates. These intermediates act as Lewis acid sites during the HC reaction. The metal species actively enhance these Lewis acid sites to improve the dehydration of ethanol, leading to increased ethylene production. The availability of more ethylene, in turn, promotes secondary reactions, leading to a broader product distribution [3].

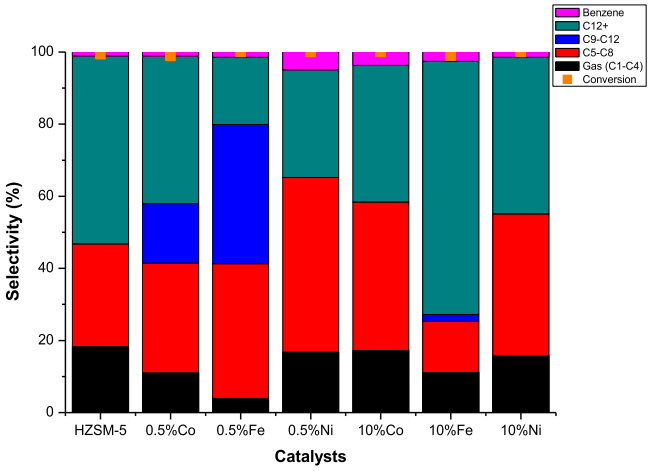

Fig. 5. Product distribution over pure and modified HZSM-5 for ethanol-to-hydrocarbon (ETH) reaction. Reaction conditions: 350 °C; WHSV=12 h^{-1}.

Among the catalysts doped with 0.5 wt%, Ni/HZSM-5 exhibited the highest selectivity for aromatics compared to the other catalysts. This can be attributed to the modification of the acid sites by incorporating Ni metal species, which led to a significant increase in the concentration of weak acid and total acid sites. This increased concentration of weak acid sites in the Ni-doped catalyst enhances the selective formation of aromatics through the formation of active sites that favour aromatisation reactions, resulting in higher aromatic selectivity compared to Co and Fe-doped catalysts that favour C_9—C_{12} HCs. Increased total and weak acid sites promote aromatic formation by aiding aromatisation during ethanol conversion to hydrocarbons [37,38]. However, a decrease in aromatic selectivity was recorded with the high (10 wt%) Ni loading. This is due to the significant presence of strong acid sites in the catalyst and the small number of weak acid sites. Strong acid sites promote undesirable side reactions such as cracking and shortening the hydrocarbon chain, which compete with aromatics formation. The increase in aromatics selectivity observed with 10 wt% Co- and Fe-doped HZSM-5 catalysts can be attributed to a slight increase in the moderate and strong acid sites compared to Ni/HZSM-5, which has a significant increase in these acid sites. Compared to the unmodified catalysts, the appreciable total acid sites in the Co- and Fe-doped catalysts provide more active sites for converting oxygenated intermediates to olefins, followed by cyclisation and aromatisation to produce aromatics. Hence, the presence of metal dopants enhances the catalytic activity of the zeolite, resulting in higher yields of aromatics. However, it should be noted that metal doping can also increase the likelihood of coke deposition and subsequent catalyst deactivation. The formation of coke is primarily caused by processes such as oligomerisation, dehydrogenation, aromatisation, and hydrogen transfer, all of which are mainly connected to the strength and quantity of acid sites on the catalyst's surface [39].

The mechanism for ETH conversion is very similar to the process of transforming methanol-to-hydrocarbons (MTH). However, the direct dehydration of ethanol to produce ethylene eliminates the need for an indirect carbon–carbon coupling pathway, including the hydrocarbon pool mechanism. In the present study, based on the product distribution, it is believed that ethanol was first dehydrated to generate ethylene and diethyl ether (DEE) by a concerted mechanism. DEE can be further cracked to produce ethylene, providing an alternative reaction pathway. Ethylene can undergo dehydrogenation to form ethyl radicals participating in secondary reaction pathways. Aromatisation reactions involve the cyclisation of carbocation intermediates, forming aromatic hydrocarbons such as benzene. ZSM-5 catalysts also facilitate the formation of long-chain hydrocarbons (C_5+) through oligomerisation reactions. These HCs are usually formed through secondary carbocation reactions or additional transformations of the intermediates generated during aromatisation [40]. The study by Niu et al. [41] also reported a similar pathway. However, the performance of ZSM-5 catalysts modified with transition metals depends on the type and concentration of the transition metal in the ZSM-5 catalyst support and the operating conditions used

for the reaction, which affect product selectivity and distribution.

3.7. Effect of transition metal modification on stability, coking and deactivation of ZSM-5

A well-known method for promoting the synthesis and performance of certain catalysts is using metal-doped zeolites in catalytic processes. Rapid deactivation of such catalysts by coke formation is among their significant technical problems. The thermal stability of the catalyst used in this study was evaluated after ethanol conversion. The initial weight loss under nitrogen flow (from $T = 0$–200 °C) was not considered in the coke calculation because the weight loss at this stage was attributed to the removal of absorbed water and other volatile compounds in the spent catalysts [42]. The pure (unused) HZSM-5 and the used HZSM-5 are denoted as HZSM-5 (pure) and HZSM-5 (spent). From $T =$ 200–800 °C, the gas flow was switched to air while maintaining the same flow rate. The weight loss at this stage is due to the decoking process (Fig. 6), and three stages of decoking were identified: stage one involves the burning of soft coke at $T = 200$–400 °C, which is a slow process. The weight loss at this stage showed that 0.5 wt% doped catalysts had the lowest percentage weight loss at 0.88, 0.59, and 1.07 wt% for 0.5 % Fe, Ni, and Co, respectively, compared to 10 % metal-loaded HZSM-5 catalyst, which had a weight loss >of 1.4 wt% at this temperature. A temperature rise of 400–600 °C triggers the second stage of coke decomposition, which consists of the burning of hard coke. Significant weight loss is observed in this stage due to the higher reaction rate, with 0.5 wt% Ni and Co showing the lowest weight loss at 2.8 wt% and 2.3 wt %, respectively, compared to 0.5 wt% Fe (4.12 %) and the unmodified catalyst (3.50 wt%).

At a higher metal doping of 10 wt%, a high weight loss was observed, especially for catalysts doped with Fe (8.70 wt%) and Ni (6.33 wt%), in contrast to Co (3.86 wt%), which showed appreciable stability with the lowest coke amount at this stage. A decrease in the amount of coke was observed in stage 3 from 600 to 800 °C, which may be attributed to the non-volatile or laid coke [42]. The catalyst loaded with 10 % metal showed the lowest weight loss in this stage. It is obvious that the pure catalyst had the lowest weight loss (1.62 wt%) since it was not subjected to any reaction, so no coke was deposited, and the weight loss can be attributed to the impurities or other organic compounds. The increase in total coke deposition is in the order HZSM-5 (pure) (1.62 wt%) < 0.5Co (4.56 wt%) < 0.5Ni (4.59 wt%) < 10Co (6.20 wt%) < HZSM-5 (spent) (6.74 wt%) < 0.5Fe (6.77 wt%) < 10Ni (8.57 wt%) < 10Fe (12.06 wt%) and results show that metal loading increasing coke deposition which increases with increased concentration. Coke deposition is closely related to the acidity of the catalyst, as shown by the observation that higher metal doping, leading to increased strong acid sites, is associated with greater coke deposition. This trend is particularly evident for catalysts modified with 10 wt% (Co, Fe, and Ni), which recorded a significant coke formation. In contrast, catalysts with lower metal doping (0.5 wt%), have a lower level of strong acid sites, resulting in reduced coke deposition.

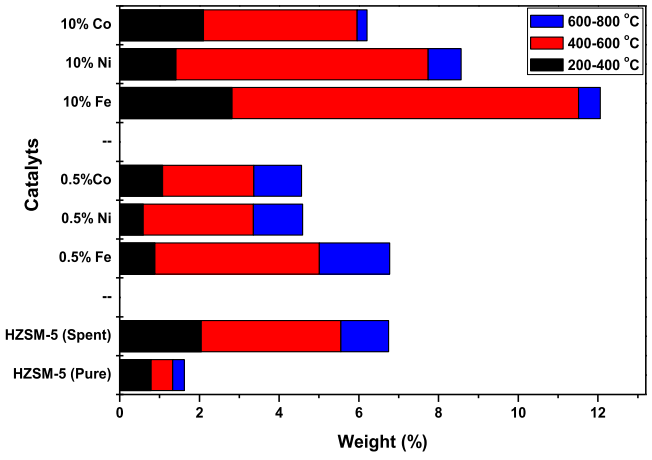

Fig. 6. Coke deposition on spent catalysts: *effect of transition metal concentration on coke formation*.

In agreement with the present study, Xu et al. [43] reported that Fe influences the ZSM-5 by forming carbonaceous deposits. However, the amounts of coke discovered by TGA increase with an increase in metal (Fe) concentration, which does not agree with the earlier result by Weckhuysen et al. [44] that coke formation is prevented by metal introduction. Although the amount of coke formed in the subsequently consumed metal-doped sample is much greater than that produced with the unmodified catalyst (5 wt%Mo/Z5), the catalyst doped with 1.0 wt% Fe shows the best consistent performance in the synthesis of benzene over the limited time. The catalysts with 0.3 wt% and 0.5 wt% Fe/(5 wt %Mo/Z5) demonstrated better performance and stability than the pure catalyst and showed that the coke formation is not reduced by the addition of Fe [43]. In the study by Persson et al. [35], it was found that metal modification promotes coke formation primarily by increasing the concentration of acid sites. In some cases, this could be due to the fact that more Brønsted acid sites promote cracking and other hydrocarbon reactions within the catalysts, accelerating coke formation. Thus, the strength of the acid sites influences how much coking occurs. Although the metal modification increases the susceptibility of the catalyst to coking, it also accelerates the oxidation of the coke and simultaneously lowers the regeneration temperature of the catalyst [45].

4. Conclusion

Zeolites are considered the preferred porous materials for heterogeneous catalysis because they have Brønsted acid sites on their surface. The results of this study show that ZSM-5 modified with transition metals does not change the characteristic peaks of the MFI framework of the ZSM-5 zeolite, but that increased metal doping (10 wt%) decreases the crystallinity of pure ZSM-5, as the presence of metal oxide peaks becomes visible at increased metal concentration. The metal-modified ZSM-5 retained the characteristic functional groups of ZSM-5, but the vibrational bands decreased with increasing metal concentration at 10 wt%. The particle size of the catalyst increases with increasing metal concentration from 0.5 to 10 wt% while the prismatic crystal shape remains unaltered. Surface area, total pore size, and pore diameter decreased with increasing metal concentration. In particular, the surface area of the pure catalysts decreased by 8.8 %, 2.6 % and 4 % for 0.5 wt% Co, Fe and Ni, while the addition of 10 wt% of these metals resulted in a more significant reduction of 19.7 %, 12.5 % and 23 %, respectively, compared to the original surface area of 397.5 m^2/g of the pure catalysts. Metal-doping increases the Lewis acid sites of the catalyst while decreasing the amount of strong acid sites. This can be attributed to the neutralisation of some parts of the Brønsted sites by forming additional Lewis acid sites. The coke study showed that increased metal doping accelerated the coke yield due to the increased acid sites. Consequently, the introduction of a low metal content (0.5 wt%) resulted in a lower coke deposition of 4.5–6.8 %, in contrast to a higher metal content (10 wt%), which resulted in a higher coke formation (6.2–12.1 %). It is noteworthy that the Co-doped catalysts exhibited remarkable stability among all catalysts. According to the catalyst test result, low metal doping (0.5 wt%) showed optimal catalytic performance with broader product distribution and less coke deposition compared to highly doped catalysts. While the Ni-doped catalysts favoured aromatics and C_5–C_9, Fe- and Co-doped catalysts preferred C_9–C_{12} and C_{12}+ HCs, respectively. Therefore, the distribution of metal species and acid sites on catalysts plays a crucial role in determining the performance and selectivity of catalysts in hydrocarbon conversion processes. It should be noted that the use of an appropriate metal content on ZSM-5 catalysts can reduce coking of the catalysts and other undesirable side reactions while increasing the selectivity of the target products.

CRediT authorship contribution statement

Ifeanyi Michael Smarte Anekwe: Data curation, Formal analysis, Investigation, Methodology, Visualization, Writing – original draft. **Bilainu Oboirien:** Supervision, Validation, Writing – review & editing, Writing – review & editing, Project administration, Conceptualization. **Yusuf Makarfi Isa:** Conceptualization, Funding acquisition, Project administration, Resources, Supervision, Validation, Writing – review & editing.

Declaration of Competing Interest

The authors declare that they have no known competing financial interests or personal relationships that could have appeared to influence the work reported in this paper.

Data availability

Data will be made available on request.

Acknowledgments

This work is financially supported by an international collaborative project (BRICS2019-040) under the BRICS STI Framework Programme with government funding organizations of South Africa NRF (BRIC190321424123), Brazil CNPq (402849/2019-1), Russia RFBR (19-58-80016), India DST (CRG/2018/004610, DST/TDT/ TDP-011/2017) and China MOST (2018YFE0183600).

Supplementary materials

Supplementary material associated with this article can be found, in the online version, at doi:10.1016/j.jfueco.2023.100101.

References

[1] Yan Z, et al. A theoretical insight into diffusion mechanism of benzene-methanol alkylation reaction in ZSM-5 zeolite. Microporous Mesoporous Mater 2022;337:111926.
[2] Kamaluddin HS, Gong X, Ma P, Narasimharao K, Chowdhury AD, Mokhtar M. Influence of zeolite ZSM-5 synthesis protocols and physicochemical properties in the methanol-to-olefin process. Mater Today Chem 2022;26:101061.
[3] Anekwe IMS, Oboirien B, Isa YM. Catalytic conversion of bioethanol over cobalt and nickel-doped HZSM-5 zeolite catalysts. Biofuels Bioprod Biorefin 2023.
[4] Zheng Y, et al. Study on aromatics production via the catalytic pyrolysis vapor upgrading of biomass using metal-loaded modified H-ZSM-5. J Anal Appl Pyrolysis 2017;126:169–79.
[5] Du Z, et al. Production of aromatic hydrocarbons by catalytic pyrolysis of microalgae with zeolites: catalyst screening in a pyroprobe. Bioresour Technol 2013;139:397–401.
[6] Persson H, Duman I, Wang S, Pettersson L, Yang W. Catalytic pyrolysis over transition metal-modified zeolites: a comparative study between catalyst activity and deactivation. J Anal Appl Pyrolysis 2019;138:54–61.
[7] ASTM. D5758-01: Standard Test Method for Determination of Relative Crystallinity of Zeolite ZSM-5 by X-Ray Diffraction. West Conshohocken, PA: ASTM International; 2011. p. 19428–2959.
[8] Ji K, et al. The study of methanol aromatization on transition metal modified ZSM-5 catalyst. Chin J Chem Eng 2018;26(9):1949–53. https://doi.org/10.1016/j.cjche.2018.03.024. 2018/09/01.
[9] Machado NRCF, Calsavara V, Astrath NGC, Matsuda CK, Paesano A, Baesso ML. Obtaining hydrocarbons from ethanol over iron-modified ZSM-5 zeolites. Fuel 2005;84(16):2064–70. https://doi.org/10.1016/j.fuel.2005.05.001. 11/01/2005.
[10] Li X, Alwakwak AA, Rezaei F, Rownaghi AA. Synthesis of Cr, Cu, Ni, and Y-doped 3D-printed ZSM-5 monoliths and their catalytic performance for n-hexane cracking. ACS Appl Energy Mater 2018;1(6):2740–8.
[11] Huo C, Ouyang J, Yang H. CuO nanoparticles encapsulated inside Al-MCM-41 mesoporous materials via direct synthetic route. Sci Rep 2014;4(1):1–9.
[12] Wu Z, et al. Mesoporous Cr_2O_3-supported Au–Pd nanoparticles: high-performance catalysts for the oxidation of toluene. Microporous Mesoporous Mater 2016;224:311–22.
[13] Mimura N, Takahara I, Inaba M, Okamoto M, Murata K. High-performance Cr/H-ZSM-5 catalysts for oxidative dehydrogenation of ethane to ethylene with CO_2 as an oxidant. Catal Commun 2002;3(6):257–62.
[14] Calsavara V, Baesso ML, Fernandes-Machado NRC. Transformation of ethanol into hydrocarbons on ZSM-5 zeolites modified with iron in different ways. Fuel 2008;87(8–9):1628–36.
[15] Saeidi M, Hamidzadeh M. Co-doping a metal (Cr, Mn, Fe, Co, Ni, Cu, and Zn) on Mn/ZSM-5 catalyst and its effect on the catalytic reduction of nitrogen oxides with ammonia. Res Chem Intermed 2017;43(4):2143–57.
[16] Seemala B, Wyman CE. Relationship between ZSM-5 pore modifications and gallium proximity and liquid hydrocarbon number distribution from ethanol oligomerization. Catal Sci Technol 2022;12(15):4903–16.
[17] Rahimi S, Yousefi MR, Rostamizadeh M. Metal-doped high silica ZSM-5 nanocatalyst for efficient conversion of plastic to value-added hydrocarbons. Polym Degrad Stab 2021;191:109653. https://doi.org/10.1016/j.polymdegradstab.2021.109653. 09/01/2021.
[18] Tong Y, Yang T, Li B, Song H, Kai X, Li R. Transition metal load HZSM-5 catalyst assisted hydrothermal conversion of sewage sludge: nitrogen transformation mechanism and denitrification effectiveness of bio-oil. J Energy Inst 2022.
[19] Kazemi Hakki H, Shekari P, Najafidoust A, Dezhvan N, Seddighi Rad M. Influence of calcination temperature and operational parameters on Fe-ZSM-5 catalyst performance in sonocatalytic degradation of phenol from wastewater. J Water Environ Nanotechnol 2021;6(2):150–63.
[20] Mohammed BBa, et al. Fe-ZSM-5 zeolite for efficient removal of basic Fuchsin dye from aqueous solutions: synthesis, characterization and adsorption process optimization using BBD-RSM modeling. J Environ Chem Eng 2020;8(5):104419. https://doi.org/10.1016/j.jece.2020.104419. 10/01/2020.
[21] Zhu Z, Lu G, Zhang Z, Guo Y, Guo Y, Wang Y. Highly active and stable Co_3O_4/ZSM-5 catalyst for propane oxidation: effect of the preparation method. ACS Catal 2013;3(6):1154–64. https://doi.org/10.1021/cs400068v. 06/07 2013.
[22] Shams-Ghahfarokhi Z, Nezamzadeh-Ejhieh A. As-synthesized ZSM-5 zeolite as a suitable support for increasing the photoactivity of semiconductors in a typical photodegradation process. Mater Sci Semicond Process 2015;39:265–75. https://doi.org/10.1016/j.mssp.2015.05.022. 11/01/2015.
[23] Feng R, et al. Two-stage glucose-assisted crystallization of ZSM-5 to improve methanol to propylene (MTP). Microporous Mesoporous Mater 2018;270:57–66. https://doi.org/10.1016/j.micromeso.2018.05.003. 11/01/2018.
[24] Hajimirzaee S, Soleimani Mehr A, Kianfar E. Modified ZSM-5 zeolite for conversion of LPG to aromatics. Polycycl Aromat Compd 2020:1–14.
[25] Sanakousar F, Vidyasagar C, Jiménez-Pérez V, Prakash K. Recent progress on visible-light-driven metal and non-metal doped ZnO nanostructures for photocatalytic degradation of organic pollutants. Mater Sci Semicond Process 2022;140:106390.
[26] Lee K, Choi B, Lee C, Oh K. Effects of SiO_2/Al_2O_3 ratio, reaction atmosphere and metal additive on de-NOx performance of HC-SCR over Cu-based ZSM-5. J Ind Eng Chem 2020;90:132–44.
[27] Li X, Rezaei F, Rownaghi AA. Methanol-to-olefin conversion on 3D-printed ZSM-5 monolith catalysts: effects of metal doping, mesoporosity and acid strength. Microporous Mesoporous Mater 2019;276:1–12. https://doi.org/10.1016/j.micromeso.2018.09.016. 03/01/2019.
[28] Rostamizadeh M, Yaripour F, Hazrati H. Ni-doped high silica HZSM-5 zeolite (Si/Al = 200) nanocatalyst for the selective production of olefins from methanol. J Anal Appl Pyrolysis 2018;132:1–10. https://doi.org/10.1016/j.jaap.2018.04.003. 06/01/2018.
[29] Saini B, Tathod AP, Diwakar J, Arumugam S, Viswanadham N. Nickel nanoparticles confined in ZSM-5 framework as an efficient catalyst for selective hydrodeoxygenation of lignin-derived monomers. Biomass Bioenergy 2022;157:106350. https://doi.org/10.1016/j.biombioe.2022.106350. 02/01/2022.
[30] Wei Z, et al. Steamed Zn/ZSM-5 catalysts for improved methanol aromatization with high stability. Fuel Process Technol 2017;162:66–77.
[31] Che Q, et al. Influence of physicochemical properties of metal modified ZSM-5 catalyst on benzene, toluene and xylene production from biomass catalytic pyrolysis. Bioresour Technol 2019;278:248–54.
[32] Rostamizadeh M, Yaripour F. Bifunctional and bimetallic Fe/ZSM-5 nanocatalysts for methanol to olefin reaction. Fuel 2016;181:537–46. https://doi.org/10.1016/j.fuel.2016.05.019. 10/01/2016.
[33] Arjah A, Al-Bahar M, Li C, Garforth A. Selective cracking of light olefins to ethene and propene. Chem Eng Trans 2017;57.
[34] Trinh QH, Lee SB, Mok YS. Removal of ethylene from air stream by adsorption and plasma-catalytic oxidation using silver-based bimetallic catalysts supported on zeolite. J Hazard Mater 2015;285:525–34.
[35] Persson H, Duman I, Wang S, Pettersson LJ, Yang W. Catalytic pyrolysis over transition metal-modified zeolites: a comparative study between catalyst activity and deactivation. J Anal Appl Pyrolysis 2019;138:54–61. https://doi.org/10.1016/j.jaap.2018.12.005. 03/01/2019.
[36] Huang X, Sun X, Zhu S, Liu Z. Benzene alkylation with propane over metal modified HZSM-5. React Kinet Catal Lett 2007;91(2):385–90.
[37] Yang M, et al. Conversion of lignin into light olefins and aromatics over Fe/ZSM-5 catalytic fast pyrolysis: significance of Fe contents and temperature. J Anal Appl Pyrolysis 2019;137:259–65.
[38] Li H, et al. Effect of the post-treatment of HZSM-5 on catalytic performance for methanol to aromatics. ChemistrySelect 2020;5(11):3413–9. https://doi.org/10.1002/slct.202000118.
[39] Akhoundzadeh H, Taghizadeh M, Pajaie HS. Synthesis of highly selective and stable mesoporous Ni–Ce/SAPO-34 nanocatalyst for methanol-to-olefin reaction: role of polar aprotic N, N-dimethylformamide solvent. Particuology 2018;40:113–22.
[40] Sun J, Wang Y. Recent advances in catalytic conversion of ethanol to chemicals. ACS Catal 2014;4(4):1078–90. https://doi.org/10.1021/cs4011343. 04/04 2014.

[41] Niu P, Ren X, Xiong D, Ding S, Li Y, Wei Z, et al. Synthesis of highly selective and stable Co-Cr/SAPO-34 catalyst for the catalytic dehydration of ethanol to ethylene. Catalysts 2020;10(7):785.
[42] Ahmed R, Sinnathamb C, Subbarao D. Kinetics of de-coking of spent reforming catalyst. J Appl Sci 2011;11(7):1225–30.
[43] Xu Y, Wang J, Suzuki Y, Zhang ZG. Improving effect of Fe additive on the catalytic stability of Mo/HZSM-5 in the methane dehydroaromatization. Catal Today 2012; 185(1):41–6. https://doi.org/10.1016/j.cattod.2011.09.026. 05/20/2012.
[44] Weckhuysen BM, Wang D, Rosynek MP, Lunsford JH. Conversion of methane to benzene over transition metal ion ZSM-5 zeolites: I. Catalytic characterization. J Catal 1998;175(2):338–46. https://doi.org/10.1006/jcat.1998.2010. 04/25/ 1998.
[45] Jiang X, Zhou J, Zhao J, Shen D. Catalytic conversion of guaiacol as a model compound for aromatic hydrocarbon production. Biomass Bioenergy 2018;111: 343–51.